J Solid State Electrochem (2003) 7: 129–133
DOI 10.1007/s10008-002-0296-1

ORIGINAL PAPER

Guo-Tao Wu · Mao-Hui Chen · Guang-Ming Zhu
Jin-Kua You · Zu-Geng Lin · Xiao-Bin Zhang

Structural characterization and electrochemical lithium insertion properties of carbon nanotubes prepared by the catalytic decomposition of methane

Received: 14 February 2002 / Accepted: 25 May 2002 / Published online: 13 July 2002

Abstract Carbon nanotubes (CNTs) were synthesized by the catalytic decomposition of methane at 773, 873 and 973 K. Structures of these carbon nanotubes were characterized by TEM, HRTEM, XRD and Raman spectra, respectively. The results showed that with the increase of preparation temperature, the d_{002} value of the CNTs decreased, while the L_a values and the degree of crystallinity of the samples increased. Electrochemical lithium insertion properties of the CNTs used as positive electrodes in CNTs/Li cells were also investigated. The first charge capacities of CNTs/Li cells were 290, 254 and 202 mAh/g for samples produced at 773, 873 and 973 K, respectively. The sample from 773 K showed a larger charge capacity, which is attributed to the accommodation of lithium at microcavities, at edges of graphitic layers and at the surface of single graphitic layers. Its potential hysteresis during Li insertion and deinsertion processes may be related to the interstitial carbon atoms.

Keywords Carbon nanotubes · Catalytic decomposition · Methane · Lithium ion batteries

Introduction

Carbon nanotubes, due to their particular morphology, structure, physical and chemical properties, are of great interest for many potential applications, especially for electrochemical storage of energy [1]. Both single-walled nanotubes (SWNTs) [2, 3, 4] and multi-walled nanotubes (MWNTs), produced by arc discharge [5] or by the pyrolysis of hydrocarbons [6, 7], have been used as negative electrodes in lithium-ion batteries so far. The effects of the preparation methods [6, 7, 8, 9] and pretreatments [6, 7, 8, 9, 10, 11] on electrochemical lithium insertion properties of carbon nanotubes were widely studied. Carbon nanotubes prepared by different methods have different structures, and pretreatments change their structures greatly, which cause changes in the electrochemical lithium insertion properties of carbon nanotubes. The slightly graphitized carbon nanotubes possess higher capacities than the theoretical value of graphite, but show 1 V hysteresis (lithium is inserted near 0 V but is deinserted at about 1 V vs. Li) [7]. The 1 V hysteresis may be related to Li atoms bonding the interstitial carbon atoms [12, 13, 14, 15], which was proposed firstly by Wang et al. [14, 15].

Over the years, using methane as the carbon source and nickel as a catalyst, production of multi-walled nanotubes [16, 17] on a large scale, at low cost and high purity, has been well developed. In this paper, the effect of the preparation temperature on the structure and lithium insertion properties of carbon nanotubes produced by above method was investigated.

Experimental

Catalytic synthesis of carbon nanotubes

Carbon nanotubes were synthesized by the nickel-catalyzed decomposition of methane at low temperature (773–973 K). The precursor of the nickel catalyst was produced by mixtures of $Ni(NO_3)_2$, $Mg(NO_3)_2$ and citric acid calcined at 973 K. Reactions were carried out in a fixed-bed flow reactor, which was composed of a ceramic boat containing 20 mg catalyst placed in a horizontal quartz tube. The precursor of the nickel catalyst was reduced in situ by a mixture of H_2 and N_2 (1:2 v/v) at a rate of 150 mL/min for 10 min at 873 K, and then CH_4 was introduced into the quartz tube at different temperatures at the rate of 20 mL/min. As-formed carbon nanotubes were held in the diluted HNO_3 for 24 h to dissolve the catalyst, then they were filtered, washed with distilled water, and dried at 423 K under vacuum.

G.-T. Wu (✉) · M.-H. Chen · G.-M. Zhu · J.-K. You · Z.-G. Lin
State Key Laboratory for Physical Chemistry of Solid Surfaces and Department of Chemistry, Xiamen University, Xiamen, 361005, P.R. China
E-mail: guotaowu@yahoo.com.cn
Tel.: +86-592-2183905
Fax: +86-592-2183905

X.-B. Zhang
Department of Materials Science and Engineering, Zhejiang University, Hangzhou, 310027, P.R. China

Structural characterization of carbon nanotubes

Carbon nanotubes were observed by a JEOL 100 CX transmission electron microscope. High-resolution images were taken by a Philips CM20 with a point-to-point resolution of 0.19 nm operated at 200 kV. The specimens for TEM were dispersed in dehydrated ethanol by ultrasound, and then dropped on Cu grids or holey carbon grids. X-ray diffraction (XRD) measurements were performed using a Rigaku D/MAX-C diffractometer operated at 40 kV and 30 mA with Cu K_α radiation (0.15406 nm). Raman spectra were excited with 30 mW of 514.5 nm radiation from an Ar-ion laser at room temperature under ambient conditions using a confocal microprobe Raman system (LabRam I) equipped with a charge-coupled device (CCD) multi-channel detector.

Electrochemical measurements

Electrochemical measurements were performed using a three-electrode test cell made of glass. The working electrode was prepared by mixing 95 wt% carbon nanotubes with 5 wt% polytetrafluoroethylene (PTFE) as binder. The obtained gum-like mixture was spread to a thin film and pressed onto a nickel mesh (5×5 mm) at 10 MPa, and then dried under vacuum for 24 h at 393 K. The electrolyte used was 1 M $LiPF_6$ dissolved in a mixed solvent of 50% ethylene carbonate (EC) and 50% diethyl carbonate (DEC) by volume. Lithium metal was used both as the counter electrode and as the reference electrode. Cell assembly operations were carried out in a glove box filled with argon gas, where water and oxygen concentrations were kept less than 3 ppm. Discharge/charge cycle testing was implemented on an Arbin BT-2043 battery test system in a voltage range from 0.005 to 3.0 V and with a constant discharge/charge rate at 40 mA/g.

Results and discussion

Morphology and microstructure of carbon nanotubes

Figure 1 gives the results of TEM observations on samples produced from methane at the low temperature range (773–973 K). It is obvious that their outer diameters are on the order of a nanometer and they have hollow cores, though the inner diameter of the samples produced at 773 K is very small.

HRTEM images in Fig. 2 show the typical microstructure of samples produced from methane at 773 K and 973 K. As shown in Fig. 2, CNTs produced from methane are composed of graphitic sheets packed at fixed angles to the central core. Wrinkled graphite sheets and an unorganized graphitic structure, where the lattice fringes are disordered, can be seen in Fig. 2a. The wrinkled graphite sheets may be caused by the existence of the interstitial carbon atoms between the aromatic planes of carbon atoms in these materials, which can enlarge the distance of the interlayer [7, 12, 13, 14, 15]. With the increase of preparation temperature, wrinkled graphite sheets and the unorganized graphitic structure decrease (see Fig. 2) and the degree of crystallinity increases, which indicates that the interstitial carbon atoms may be destroyed.

The XRD patterns of the samples are shown in Fig. 3. The sharp and high [002] carbon Bragg peak can be seen in the patterns of all samples. The d_{002} value and crystallite size L_c are determined from the [002] carbon

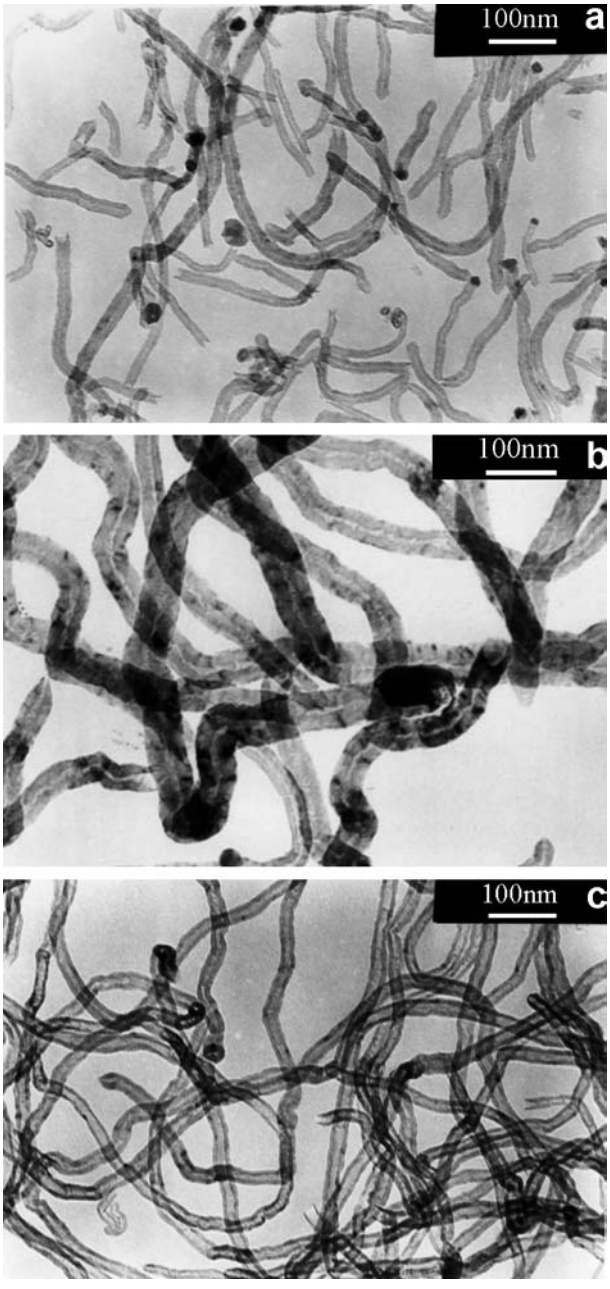

Fig. 1 TEM images of carbon nanotubes: **a** sample from 773 K; **b** sample from 873 K; **c** sample from 973 K

Bragg peak using the Bragg and Scherer formulas, $d_{002} = \lambda/2\sin\theta$ and $L_c = K\lambda/\beta\cos\theta$, where λ is the X-ray wavelength, θ is the Bragg angle, β is the real half-peak width, and the form factor K is 0.9 for L_c. The calculated L_c values are 5.1, 7.2 and 5.6 nm for samples produced at 773, 873 and 973 K, respectively. The larger L_c value for the sample produced at 873 K is associated with the larger diameter of the sample, as is confirmed by TEM observations. The calculated d_{002} values are 0.3449, 0.3415 and 0.3408 nm for samples produced at 773, 873 and 973 K, respectively. The decreasing d_{002} value of the samples with the increase of preparation temperature also confirms that the interstitial carbon atoms may be

destroyed. From XRD patterns and HRTEM images, it can be concluded that interstitial carbon atoms exist between the aromatic planes of samples produced at 773 K and the degree of crystallinity of the samples increases with the increase of preparation temperature.

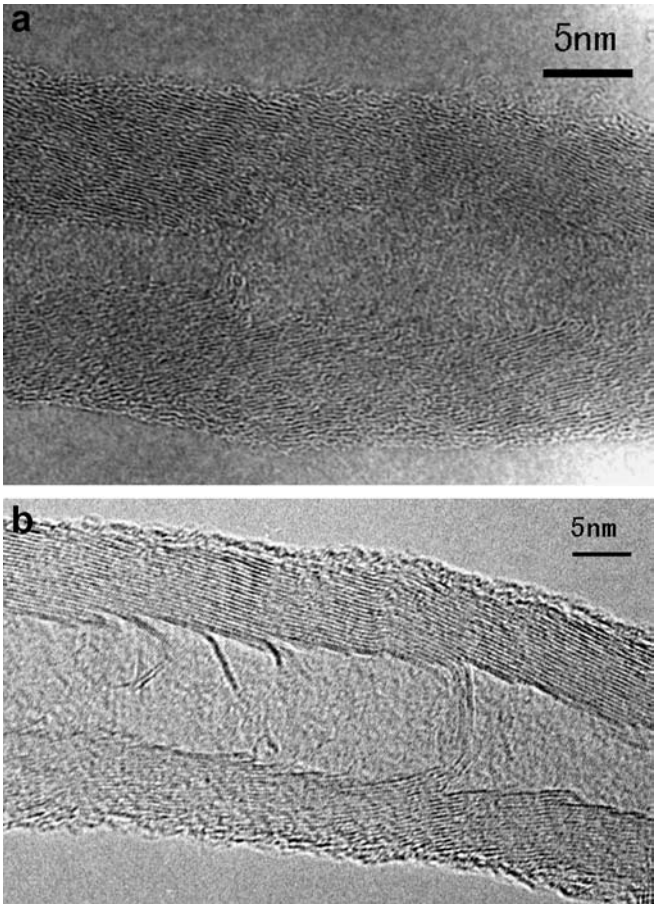

Fig. 2 HRTEM images of carbon nanotubes: **a** sample from 773 K; **b** sample from 973 K

Raman spectroscopy is a powerful and sensitive technique for studying the structure of carbonaceous material. Raman spectra of multi-wall carbon nanotubes [18] exhibited two lines at about 1350 cm^{-1} and 1580 cm^{-1}. The Raman line at 1580 cm^{-1} is often designated as the G line, and the line at 1350 cm^{-1} is designated as the D line [19]. In some cases, an additional line at 1620 cm^{-1} is found in Raman spectra, which is designated as the D′ line [20, 21, 22]. The first-order Raman scattering spectra of the samples are displayed in Fig. 4. The features of the Raman spectra, including the wave numbers and relative integrated intensities, are very similar to those of graphite with finite-size crystals, which indicates that the graphitization degree of these carbon nanotubes is relatively low [20]. Tuinstra and Koening [19] suggested that for polycrystalline graphite the intensity ratio of the 1350 cm^{-1} line and the 1580 cm^{-1} line ($R = I_D/I_G$) was inversely proportional to the effective crystallite size in the direction of the graphite plane (L_a). Here, the R values were computed either directly from the spectra or derived from the band parameters calculated in the fitting process. The computed R values are 2.06, 1.63 and 1.53 for samples produced at 773, 873 and 973 K, respectively. With the increase of preparation temperature, the R values of the samples decrease, and the L_a values of the samples increase. Furthermore, from Fig. 4 it is found that the Raman line near 1580 cm^{-1} for the samples produced at 773 K shifts from 1580 cm^{-1} to 1590 cm^{-1}. The shift is associated with an additional Raman line at 1620 cm^{-1}, which seems to arise from the vibration of carbon-carbon atoms near the interstitial carbon atom [7, 14, 15]. With the increase of preparation temperature, the interstitial carbon atoms decrease, the relative intensity of the 1620 cm^{-1} line decreases, and the Raman line near 1580 cm^{-1} shifts back, which also agrees with the existence of interstitial carbon atoms between the aromatic planes of samples produced at 773 K.

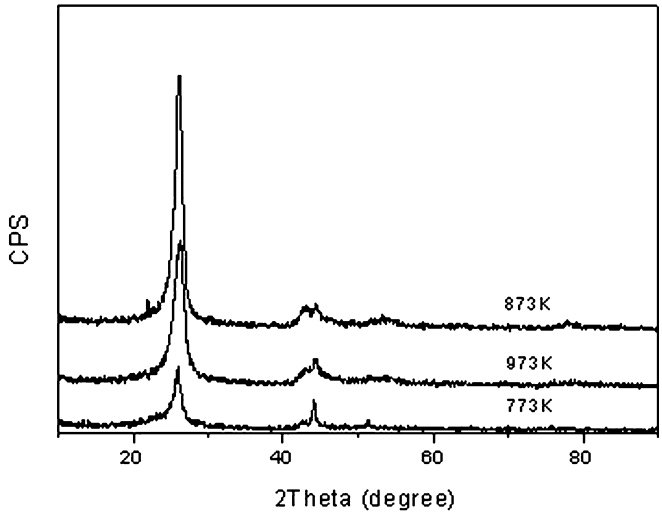

Fig. 3 XRD patterns of carbon nanotubes

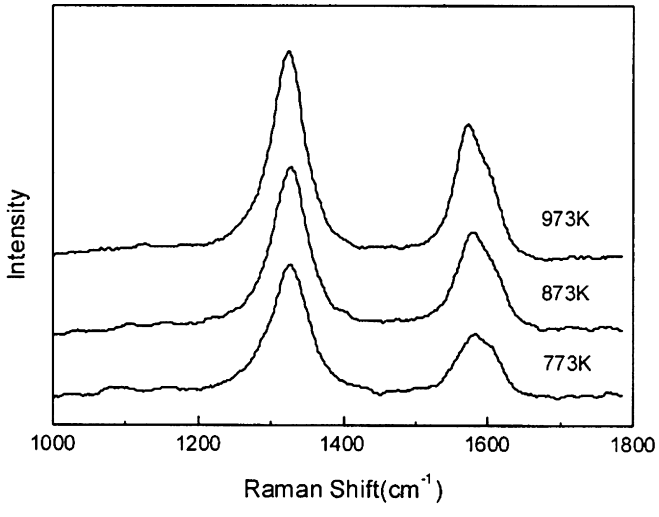

Fig. 4 Raman spectra of carbon nanotubes

Discharge and charge at the carbon nanotubes electrode

Figure 5 shows the first and subsequent discharge/charge curves for carbon nanotubes/Li cells. In the present research, the discharge curves correspond to an intercalation process and the charge curves to a deintercalation process, because the carbon nanotubes electrode is positive to the counter electrode of lithium metal. The plateau at about 0.8 V in the first discharge curves may be related to the formation of a passivation film or solid electrolyte interphase (SEI) on the carbon surface. After this passivation, Li can insert reversibly into the samples. The first charge capacities of carbon nanotubes/Li cells are 290, 254 and 202 mAh/g for samples produced at 773, 873 and 973 K, respectively, and then different samples show different potential profiles. As shown in Fig. 5, the potential profiles of samples produced at 773 K show a large hysteresis, i.e. the lithium was inserted below 0.25 V and deinserted above 1 V, but the potential profiles of samples produced at 873 K and 973 K do not show the hysteresis, which indicates that their mechanisms of lithium insertion are different. According to the potential profiles, the mechanism of lithium insertion into samples produced at 873 K and 973 K may be similar to that of graphite: lithium is intercalated into the interlayer of graphite planes. However, the high charge capacity of samples produced at 773 K may be related to the Li doped mainly into microcavities [23, 24], the edges of graphitic layers [25] and the surface of single graphitic layers [26], besides lithium insertion into the interlayer of graphite planes.

To show the effects of lithium insertion into different sites, the first charge capacities are divided into two voltage ranges, 0–1 V and 1–3 V vs. Li. The capacity in the ranges of 0–1 V may be attributed to lithium insertion into the interlayer of graphite planes. The capacity in the ranges of 1–3 V may be attributed to Li doped mainly into microcavities, the edges of graphitic layers and the surface of single graphitic layers [26]. As shown in Table 1, the first charge capacity below 1 V for samples produced at 873 K is higher than that for samples produced at 973 K, which may be due to the larger L_c value of the samples produced at 873 K. For the sample produced at 773 K, the first charge capacity above 1 V is higher than that for samples produced at 873 K and 973 K. Its mechanism of lithium insertion may be similar to that of high-capacity carbon with a large hysteresis. It has been proposed that the excess capacity may be related to the Li doped mainly into microcavities, the edges of graphitic layers and the surface of single graphitic layers. As the Raman spectra, XRD and HRTEM of the sample produced at 773 K showed that there exist interstitial carbon atoms between the aromatic planes, we believe that its potential hysteresis can be attributed to the interstitial carbon atoms as mentioned in our previous papers [7, 14, 15].

However, the cycle life of the sample produced at 773 K appears to be limited compared with those produced at 873 K and 973 K. Figure 6 shows the charge capacity versus cycle number of the Li/carbon nanotubes cells. The charge capacity of the sample produced at 773 K degrades quickly during the first three cycles. The capacity loss is mainly due to elimination of the capacity

Table 1 First discharge and charge capacities of carbon nanotubes/Li cells[a]

Sample	773 K	873 K	973 K
First discharge capacity (mAh/g)	1032	905	609
First charge capacity (mAh/g)	290	254	202
First charge capacity, 0–1 V (mAh/g)	150	200	136
First charge capacity, 1–3 V (mAh/g)	140	54	56

[a]First charge capacities are given in two voltage ranges

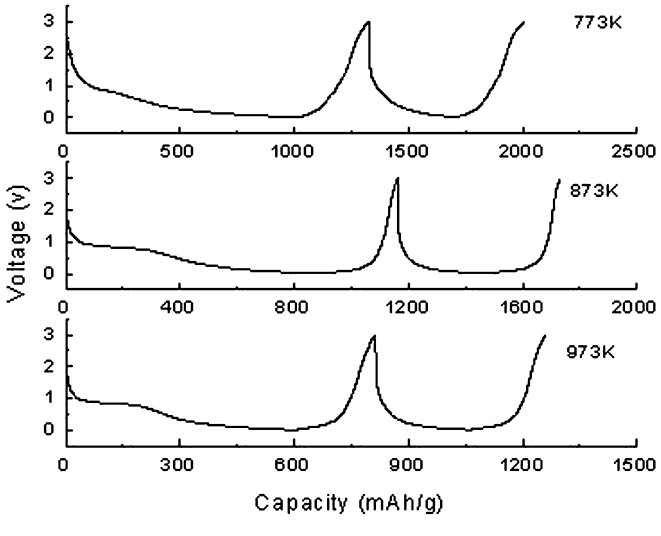

Fig. 5 The first and subsequent discharge/charge curves of carbon nanotubes/Li cells

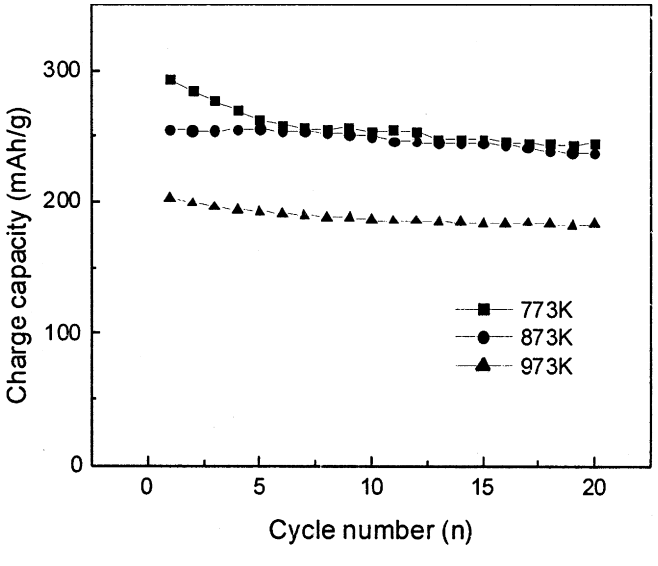

Fig. 6 Charge capacity versus cycle number for cells made from carbon nanotubes

above 1 V, which can be understood as some vacancies and microcavities being destroyed by interstitial carbons or lithium during the Li insertion and deinsertion processes.

Conclusions

Carbon nanotubes were prepared by nickel-catalyzed decomposition of methane at low temperature (773–973 K). The effects of preparation temperature on the structure and lithium insertion properties of the carbon nanotubes were investigated. The XRD, HRTEM and Raman spectra showed that, with the increase of preparation temperature, the d_{002} values of the samples decreased, the L_a values of the samples increased and the degree of crystallinity of the samples increased. The results of electrochemical measurements showed that the first charge capacity of the carbon nanotubes decreased with the increase of preparation temperature. The sample produced at 773 K showed a larger charge capacity and larger hysteresis. The higher charge capacity of the sample produced at 773 K is attributed to the extra Li doped into microcavities, the edges of graphitic layers and the surface of single graphitic layers in addition to the interlayer of graphite planes. The hysteresis during the Li insertion and deinsertion processes may be also related to the interstitial carbon atoms.

Acknowledgements The authors acknowledge the financial support from the National Natural Science Foundation of China (no. 59872030) and the National Natural Science Foundation of Fujian Province (no. E0010002).

References

1. Che GL, Lakshmi BB, Fisher ER, Martin CR (1998) Nature 393:346
2. Gao B, Kleinhammes A, Tang XP, Bower C, Fleming L, Wu Y, Zhou O (1999) Chem Phys Lett 307:153
3. Claye AS, Fischer JE, Huffman CB, Rinzler AG, Smalley RE (2000) J Electrochem Soc 147:2845
4. Barisci JN, Wallace GG, Baughman RH (2000) J Electrochem Soc 147:4580
5. Maurin G, Bousquet C, Henn F, Bernier P, Almairac R, Simon B (1999) Chem Phys Lett 312:14
6. Frackowiak E, Gautier S, Gaucher H, Bonnamy S, Beguin F (1999) Carbon 37:61
7. Wu GT, Wang CS, Zhang XB, Yang HS, Qi ZF, He PM, Li WZ (1999) J Electrochem Soc 146:1696
8. Isihara T, Fukunaga A, Akiyoshi R, Yoshio M, Takita Y (2000) Denki Kagaku 68:38
9. Beguin F, Metenier K, Pellenq R, Bonnamy S, Frackowiak E (2000) Mol Cryst Liq Cryst 340:547
10. Leroux F, Metenier K, Gautier S, Frackowiak E, Bonnamy S, Beguin F (1999) J Power Sources 82:317
11. Gao B, Bower C, Lorentzen JD, Fleming L, Kleinhammes A, Tang XP, McNeil LE, Wu Y, Zhou O (2000) Chem Phys Lett 327:69
12. Lachter J, Bragg RH (1986) Phys Rev B 33:8903
13. Abrahamson J, Maclagan RGA (1984) Carbon 22:291
14. Wang CS, Wu GT, Zhang XB, Qi ZF, Li WZ (1998) J Electrochem Soc 145:2751
15. Wang CS, Wu GT, Li WZ (1998) J Power Sources 76:1
16. Chen P, Zhang HB, Lin GD, Hong Q, Tsai KR (1997) Carbon 35:1495
17. Cui S, Lu CZ, Qiao YL, Cui L (1999) Carbon 37:2070
18. Kastner J, Pichler T, Kuzmany H, Curran S, Blau W, Weldon DN, Delamesiere M, Draper S, Zandbergen H (1993) Chem Phys Lett 221:53
19. Tuinstra F, Koenig JL (1970) J Chem Soc 53:1126
20. Nemanich RJ, Solin SA (1979) Phys Rev B 20:392
21. Nakamizo M, Tamai K (1984) Carbon 22:197
22. Dresselhaus MS, Dresselhaus G (1981) Adv Phys 30:290
23. Mabuchi A, Tokumitsu K, Fujimoto H, Kasuh T (1995) J Electrochem Soc 142:1041
24. Tokumitsu K, Mabuchi A, Fujimoto H, Kasuh T (1996) J Electrochem Soc 143:2235
25. Matsumura Y, Wang S, Mondori J (1995) Carbon 33:1457
26. Dahn JR, Zheng T, Liu Y, Xue JS (1995) Science 270:590